Finding fault in a shear zone: a magnetic and drill core study in the Valentine Lake Property, Newfoundland, Canada

Marie Flanagan[1], Alison Leitch[1], and Adam Wall[2]

1. Department of Earth Sciences, Memorial University of Newfoundland and Labrador, St. John's Newfoundland and Labrador A1B 3X5, Canada
2. Marathon Gold Corporation, Grand Falls-Windsor, Newfoundland and Labrador A2B 1K9, Canada
*Corresponding author: <aleitch@mun.ca>

Date received: 18 July 2022 ¶ Date accepted: 18 August 2023

ABSTRACT

The Valentine Lake Property in southwestern Newfoundland has five known gold deposits over a distance of 20 km along a northeast to southwest trend and is expected to be the future site for the largest gold mine in Atlantic Canada. The property contains structurally controlled orogenic-type quartz-tourmaline-pyrite veins, which are gold-bearing, occurring along or proximal to the Valentine Lake Shear Zone. The mineralization is found mostly on the northwest side of the shear zone in intrusive rocks and is rare in the conglomerate on the southeast side. The area has many mafic dykes, which show up well when conducting a magnetic survey due to their magnetite content. These dykes, like the mineralization, occur mainly in the intrusive rocks and trend predominantly subparallel to the shear zone, and so can help indicate structure. To constrain the location of the shear zone (and hence the mineralized region) in an area where an offset was suspected, a detailed magnetic survey was conducted over a 200 m x 300 m grid comprising sixteen lines. With the collected data, residual magnetic intensity maps were created and processed. A region was identified where the pattern of linear magnetic highs weaken and appear to terminate near the suspected offset. In combination with drill core information, this location is interpreted as a fault offset of the shear zone. The loss in magnetic intensity is possibly due to alteration or thinning of the mafic dykes near the fault.

RÉSUMÉ

La propriété du lac Valentine dans le sud-ouest de Terre-Neuve abrite cinq gîtes aurifères connus sur une distance de 20 km le long d'un axe du nord-est au sud-ouest et on anticipe qu'elle constituera l'emplacement de la plus vaste mine d'or au Canada atlantique. La propriété recèle des filons de quartz-tourmaline-pyrite orogéniques régis par la structure le long ou à proximité de la zone de cisaillement du lac Valentine. La minéralisation est principalement présente sur le flanc nord-ouest de la zone de cisaillement dans des roches intrusives et elle est rare dans le conglomérat sur le flanc méridional. Le secteur renferme de nombreux dykes mafiques, qui sont bien apparents lorsqu'on effectue un levé magnétique en raison de leur teneur magnétique. Ces dykes, à l'instar de la minéralisation, se manifestent surtout dans les roches intrusives et l'axe essentiellement subparallèles à la zone de cisaillement, et ils peuvent par conséquent faciliter l'élucidation de la structure. Pour circonscrire l'emplacement de la zone de cisaillement (et en conséquence la région minéralisée) dans un secteur où l'on soupçonnait un rejet, on a réalisé un levé magnétique détaillé suivant une grille de 200 m sur 300 constituée de 16 lignes. Les données recueillies ont permis la création et le traitement de cartes de l'intensité magnétique. On a alors repéré une région où la configuration des crêtes magnétiques linéaires s'estompe et semble prendre fin près du rejet soupçonné. Les données, conjuguées à l'information obtenue de carottes de forage, nous amènent à interpréter l'endroit comme un rejet vertical de la zone de cisaillement. L'affaiblissement de l'intensité magnétique est possiblement dû à une altération ou un amincissement des dykes mafiques près de la faille.

[Traduit par la redaction]

doi: 10.4138/atlgeo.2023.008

INTRODUCTION

The Valentine Lake Property (Fig. 1) is located about 55 km southwest of Millertown in southwestern Newfoundland and is accessible by gravel road from the town. The property has five known gold deposits over 20 km along a northeast to southwest trend: Victory, Marathon, Berry, Sprite, and Leprechaun (Fig. 1; Marathon Gold 2022). It is a future site for an open-pit gold mine which, upon completion, is expected to be the largest gold mine in Atlantic Canada with an estimated mine life of 14.3 years (Marathon Gold 2021). The property has total proven and probable mineral reserves of 51.6 Mt with a diluted gold grade of 1.62 g/t and a contained metal value of 2.7 Moz (Marathon Gold 2022, p 11).

The property contains orogenic-type quartz-tourma-line-pyrite (QtP) veins which are gold-bearing. The veins are structurally controlled and occur along or proximal to the Valentine Lake Shear Zone (VLSZ). These veins occur on the northwest side of the shear zone in intrusive rocks and are rare in the conglomerate on the southeast side. The area has several generations of mafic dykes, many of

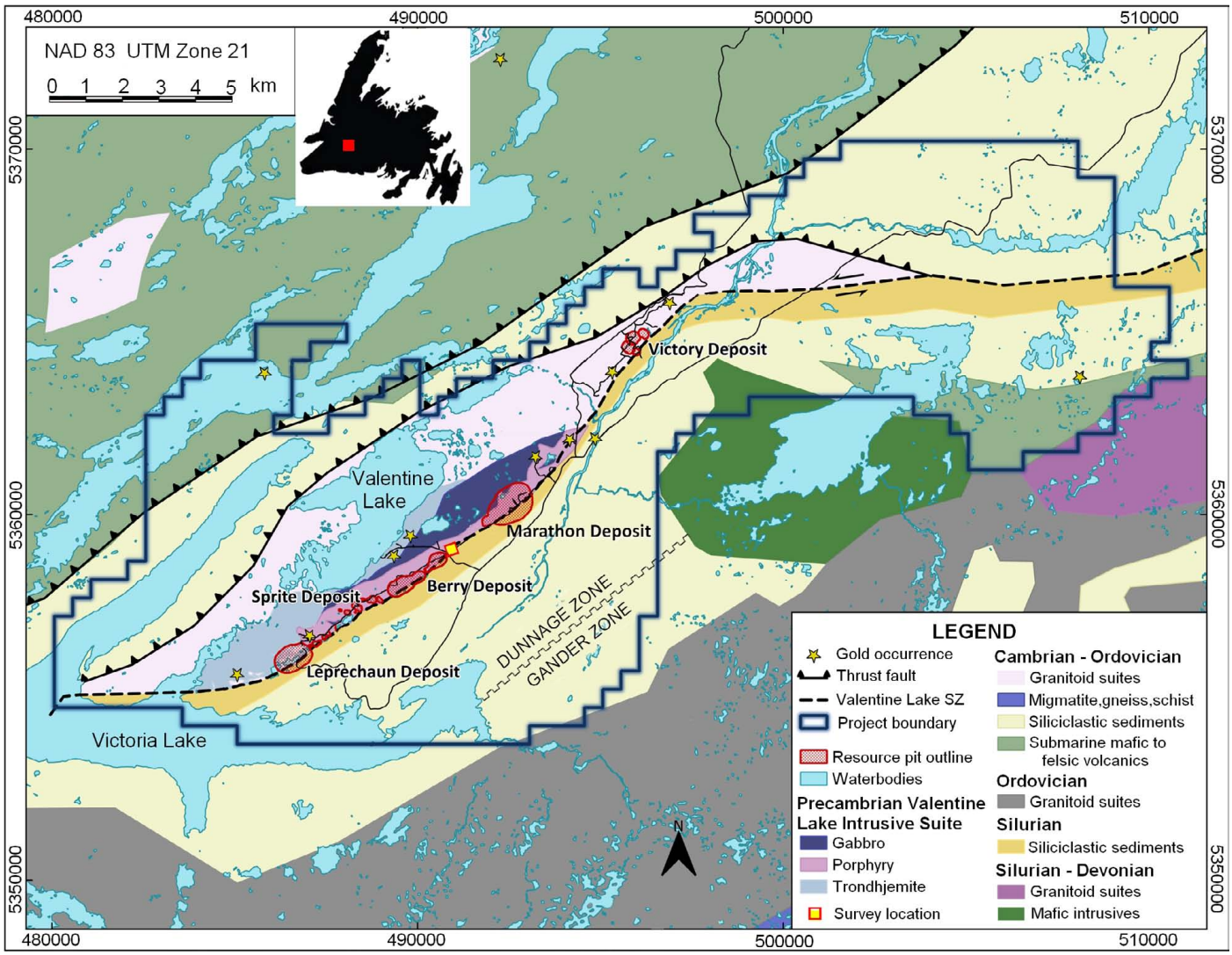

Figure 1. Geological map and location of the Valentine Lake Property in Newfoundland (red square within inset). Thin black lines indicate mining and access roads. The study area is denoted by the small yellow square to the northeast of the Berry Deposit (modified from map provided by Marathon Gold 2022).

which show up in magnetic surveys due to their magnetite content. The dykes are mostly subparallel to the VLSZ.

A ground magnetic survey was completed in 2014 that helped to identify the location of the VLSZ. In this paper we report the results of a smaller-scale, higher resolution survey that was conducted to further constrain the location of the shear zone in an area where the earlier magnetic survey and drill hole geological logs suggested that an offset may occur. The study area is located near the intersection of two access roads, northeast of the Berry Deposit (Fig. 1). As part of this study, magnetic susceptibility measurements of surrounding rock types were taken, and compared to susceptibilities measured on drill core. Total magnetic intensity maps were made and processed. The magnetic maps and magnetic susceptibility measurements were used along with drill hole geological logs from the survey area to assist in the construction of a three-dimensional model of the structure.

GEOLOGICAL SETTING

The island of Newfoundland was assembled in three orogenic episodes (Taconic, Salinic, and Acadian) during the Ordovician through Devonian, and traditionally consists of four main tectonostratigraphic zones – Humber, Dunnage, Gander, and Avalon (Fig. 2; Williams 1979). The Dunnage Zone is subdivided into the peri-Laurentian Notre Dame subzone and the peri-Gondwanan Exploits subzone (Fig. 2; Williams *et al.* 1988). The Valentine Lake property is located in the western part of the Exploits subzone, near the boundary with the Meelpaeg subzone of the Gander Zone (Figs. 1, 2).

More recent interpretations (e.g., van Staal *et al.* 2009) identified the Exploits subzone near the Valentine Lake property as the leading edge of the ribbon continent of Ganderia. This leading edge, the Victoria Arc, accreted to peri-Laurentia in the late Ordovician. It was separated from the main Gander Zone margin by the Tetagouche–Exploits backarc basin just before Ganderia collided with Laurentia in the early Silurian Salinic orogeny. This collisional event — involving the closure of the Tetagouche–Exploits backarc basin, and subsequent slab break-off — is key to understanding the structure and composition of rocks in the Valentine Lake property. No imprint of the Ordovician Taconic orogeny has been noted in the Valentine Lake property.

The VLSZ, which extends through the middle of the property (Fig. 1), is a significant structural boundary where fault systems change vergence. To the northwest of the VLSZ a series of fault splays dip steeply to the northwest. They are interpreted to have formed in the Silurian Salinic orogeny and been reactivated in the Early Devonian Acadian orogeny (Honsberger *et al.* 2022), when Avalonia was accreted onto the Laurentian margin (van Staal *et al.* 2009). The granitoid rocks of the Valentine Lake Intrusive Suite (VLIS; Fig. 1), dated as ca. 575 Ma (G. Dunning, personal communication 2022) to 565 Ma (Evans *et al.* 1990), are the oldest rocks on the Valentine Lake Property and are interpreted as peri-Gondwanan (i.e., Ganderian) basement from within the Victoria Arc. Other rocks are mainly Cambrian to Ordovician oceanic sedimentary and oceanic-arc volcanic rocks (Evans and Kean 2002; Fig. 1).

The closure of the Tetagouche–Exploits backarc basin involved west-dipping subduction under the Victoria Arc (van Staal *et al.* 2009). Subsequent break-off of the subducted slab led to a transient period (ca. 422–420 Ma) of lithospheric extension, bimodal magmatism, uplift, and erosion (Honsberger *et al.* 2022). It was during this period that the Rogerson Lake Conglomerate (RLC) and related sandstone were deposited. Mafic dykes may have been intruded into the VLIS as part of the extensional event (Kruse 2020; Honsberger *et al.* 2022). This event was followed by sinistral transpression and the generation of southeast-dipping fault splays during the Silurian-Devonian Acadian orogeny. In most places on the property, the RLC (Silurian siliciclastic sediments in Figure 1) is now overturned (younging to the southeast) in sheared, unconformable contact with the VLIS. Gold mineralization is focussed in the triangular zone where the oppositely verging fault systems meet and occurs in extensional quartz vein systems interpreted to have form in a deforming shear zone dated at ca. 410 Ma (Honsberger *et al.* 2022).

Late brittle faults, reactivating or cross-cutting earlier structures, have been associated with the Early Devonian to Carboniferous Neoacadian orogeny (Kruse 2020), which involved accretion of the Meguma terrane (van Staal *et al.* 2009).

Gold mineralization on the Valentine Lake Property is typically located within a few hundred metres northwest of the VLSZ in packages up to 100 m wide. The VLIS rocks in those areas are composed dominantly of quartz porphyry (QP) and trondhjemite. The mineralization occurs dominantly in en echelon extensional QTP veins that dip shallowly to the southwest, as well as in three other accessory vein sets at different structural orientations (Kruse 2020; Honsberger *et al.* 2022). The QTP veins vary significantly in thickness but are typically between 2 and 30 cm thick. Visible gold occurs on the sub-millimetre to millimetre scale typically within or along the margins of coarse-grained cubic pyrite in the veins.

Aeromagnetic data for the region reveal a southwest- to northeast-trending magnetic pattern following the lithology (Valverde-Vaquero and van Staal 2002). The RLC shows up as a magnetic low and a magnetic high extends along the VLIS side of the VLSZ. In 2007, a former operator of the project site, Richmont Mines Inc., completed a more detailed property-scale aeromagnetic survey (Guay *et al.* 2007). The total magnetic field map made from the survey results (Fig. 3) confirms magnetic highs extending along the VLSZ within the VLIS, associated with known deposits (black triangles).

The magnetic highs are associated with mafic dykes. The

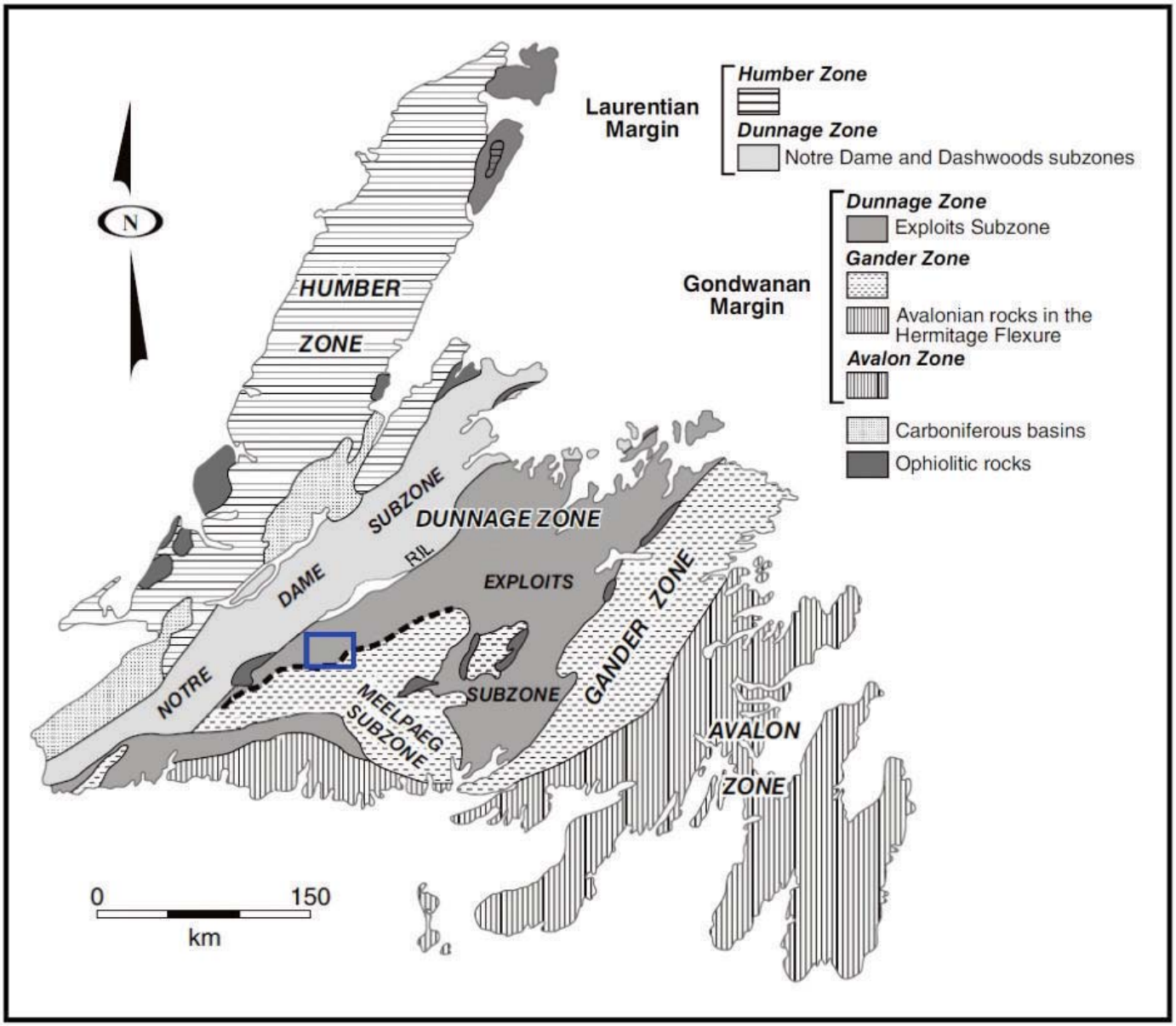

Figure 2. A generalized map of Newfoundland indicating tectonostratigraphic zones and subzones after van Staal and Valverde-Vaquero (2001), modified after Williams *et al.* (1988). The blue rectangle outlines the area covered in Figure 1. The Red Indian Line (RIL) was referred to as the Mekwe'jit Line by White and Waldron (2022).

main dyke set is orientated subparallel to the VLSZ and dips steeply to the northwest (Kruse 2020). Kruse (2020) observed that mafic dykes are typically more strongly foliated than host granitoid rocks, suggesting that the dykes were rheologically weaker. Structural analysis and field observations (Kruse 2020) indicate that the mineralized quartz veins were emplaced after the dykes: the veins are more weakly deformed than the dykes and two of the three sets of veins pinch out at the contact with dykes or propagate only a few centimeters into their sheared margins. The third vein set commonly occurs at the contact between dykes and host rock, suggesting to Kruse (2020) that their competency contrast was exploited when the veins were emplaced.

The magnetic highs to the northwest of the VLSZ are due to additional mafic dykes and gabbro bodies in the VLIS. To the southeast and south, Ordovician mafic rocks, ranging from gabbro to pillow basalt, generate elongate magnetic highs (van Staal *et al.* 2005).

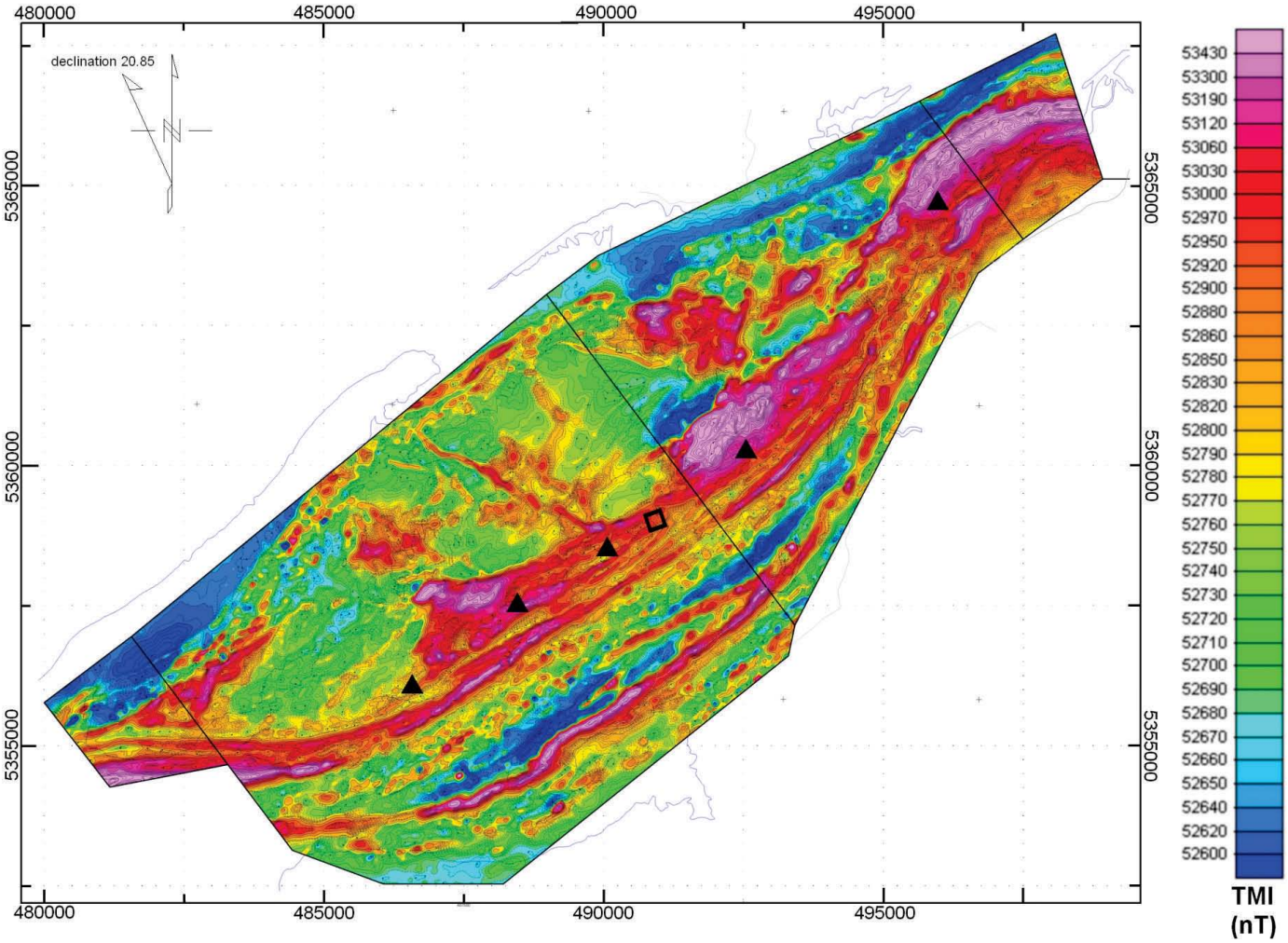

Figure 3. Airborne total magnetic intensity map of Valentine Lake Property - western part modified from Guay *et al.* (2007). Survey was done by a Bell 206L helicopter at height of 60 m, line spacing 100 m, and average speed of 23 m/s. Measurements were made using a Geometrics G-823A caesium vapour magnetometer with three sensors. Symbols: square = study area; triangles = known deposits. The conglomerate marking the Valentine Lake Shear Zone is the elongate low magnetic feature SE of the deposits.

INFORMATION FROM PREVIOUS SURVEYS

In 2014, one of us (Adam Wall, then senior geologist for Marathon Gold Corporation) carried out a ground magnetic survey over the VLSZ boundary, spanning the entire property (Fig. 4; Tettelaar and Dunsworth 2015, 2016). Many linear features with high total magnetic intensities were resolved, specifically along a similar trend as the shear zone. Structure and lithologies in the area of the 2014 ground survey are not able to be identified in outcrop due to thick vegetation and overburden, which is typically 1 to 6 m thick and up to 16 m thick in places. At the location of the yellow box (inset, Fig. 4), the linear magnetic features abruptly terminate, and a fault intersection was recorded in drill cores. In fact, one drill was stopped as a result of hitting a highly fractured region. The abrupt change in the pattern of magnetic anomalies likely corresponds to a fault that cuts the survey area. Hence this area was selected for a higher resolution ground magnetic survey.

On June 6th and 7th 2019, Light Detection and Ranging (LiDAR) elevation data were collected over the property (Melanson and Parks 2019). The data were processed before being acquired by Marathon Gold Corporation and the authors of this paper and provided one elevation reading per square metre. The LiDAR data over the survey area are shown on Figure 5. One goal of using LiDAR data was to search for any topographic indication of the postulated fault. Late brittle faults, typically subparallel to the VLSZ, are

recognized on the property, although they are not generally well exposed at surface (Kruse 2020). One E-W trending steep fault, in the Berry Zone about 1.4 km SW of the present study site, was recognized by a sinistral magnetic offset and a drill intercept (hole VL-20-827), and was found to be associated with a gouge zone visible in LiDAR data (Kruse 2020) (dotted line in Figure 4). However, at our study site the only obvious features on the map, aside from the smooth slope, are small changes in elevation along the roads. The rough surface texture under the wooded areas is generated by elevation fluctuations of about 10 cm. The south end of the survey area has an approximate elevation of 412 m above sea level and descends smoothly toward the northern end of the survey area, where the approximate elevation is 388 m.

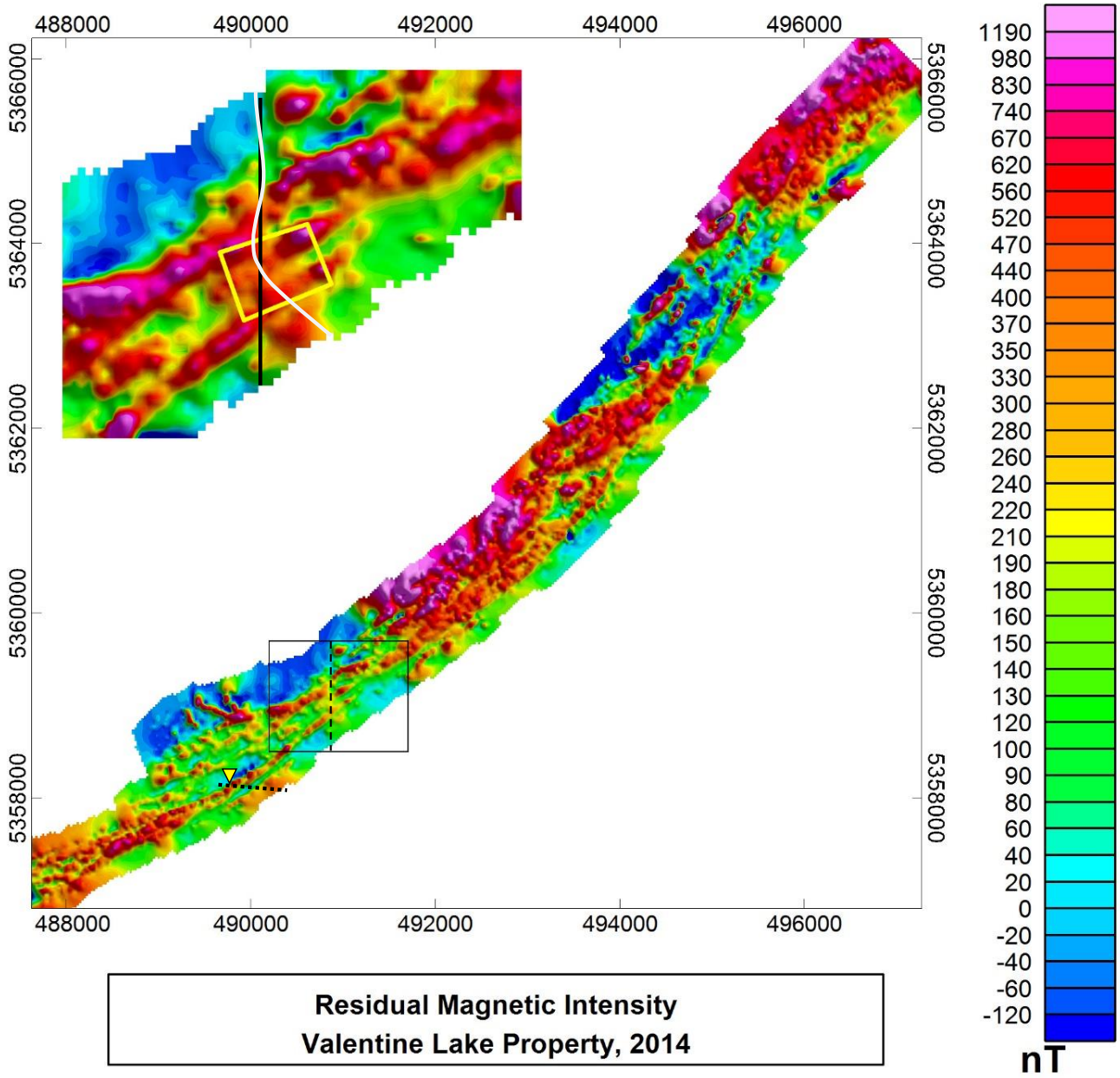

Figure 4. Residual total magnetic intensity map from a 2014 ground magnetic survey compiled from lines orientated SE to NW with a line spacing of 50 m, carried out by Adam Wall. Black rectangle indicates the area of the inset, with dashed line the location of a possible fault trace. Inset: Yellow box shows survey area for present study; grey and black lines indicate possible locations for a fault trace, based on the present study; dotted line in the SW corner indicates a sinistral fault intercepted in drill core (VL-20-827, yellow triangle) and delineated from magnetic and LiDAR data (Kruse 2020).

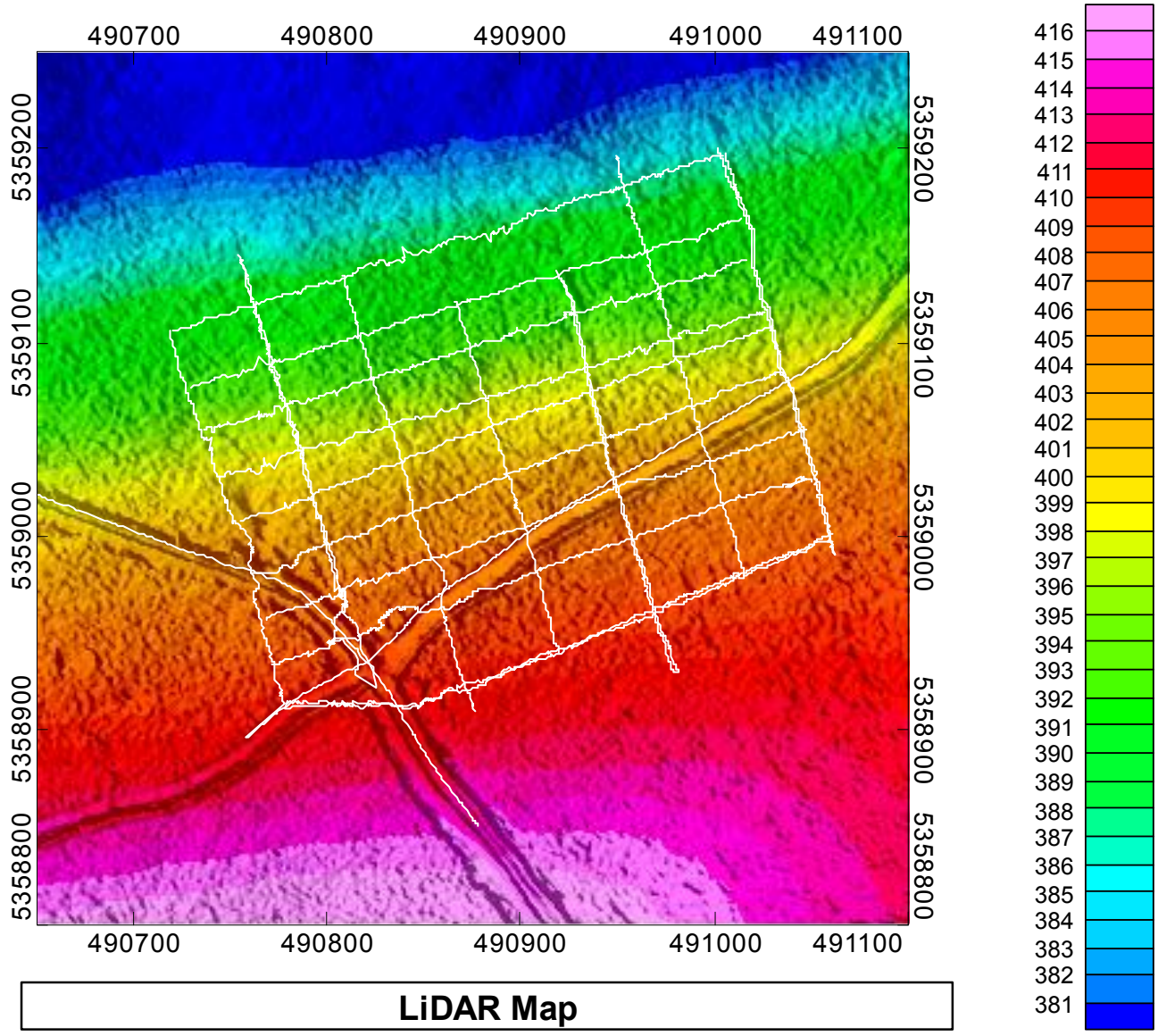

Figure 5. Elevation map from subset of LiDAR data. A Bell 206 helicopter surveyed the 63.8 km^2 property in 3 flights of 31 flight lines at 1000 ft (333 m) above ground level at a speed of 40 knots (74 km/hour) while a GPS base station logged continuously at a 1 s interval. LiDAR data were collected using a Riegl VUX-1LR scanner operating at 400 kHz, which resulted in an overall ground point density of 20.3 points/m^3 (Melanson and Parks 2019). Map using Oasis Montaj: minimum curvature gridding, 1 m cell size, and linear colour method, with shadows. Locations of grid lines and surveyed roads (white lines) were obtained from the magnetometer's GPS system.

DRILL DATA

Marathon Gold Corporation provided geological logs of ten drill cores collected in and around the survey area between 2018 and 2019 (Table 1). The cores range from 24.5 to 302 m in length. The collar locations relative to the proposed survey grid are shown in Figure 6. The main lithologies in the drill cores are overburden, quartz porphyry, mafic dykes, and conglomerate. The drill core data, with these lithologies indicated, are displayed in 3D using Leapfrog Geo® software (Fig. 7). Fault intersections are also indicated. From the drill core logs, the overburden thickness, converted from slant depths, varies from 4.2 to 8.8 m (average 6.5 m).

Table 1. Drill hole locations, orientations, and slant depths.

Hole ID	Easting (m)	Northing (m)	Elevation (m)	Depth (m)	Dip (°)	Azimuth (°)
MA-18-292	490754.99	5358987.96	405.55	140	-45.5	162.2
MA-18-293	490835.93	5359065.21	400.11	24.5	-45.00	163.5
MA-18-294	490917.66	5359136.21	390.75	41	-44.6	161.5
VL-18-675	490665.99	5358932.94	405.40	179	-45.2	163.8
VL-19-771	490624.08	5358865.62	411.99	134	-45.2	163.0
MAS-20-022	490799.1	5359182.5	382.31	302	-45.5	163.6
MAS-20-019	490971.83	5359131.1	392.75	251	-45.0	342.8
MAS-20-014	490916.58	5359119.48	393.19	185	-69.3	342.2
MAS-20-010	490743.95	5359125.91	388.21	293	-44.4	162.7
MAS-20-017	490886.72	5359233.03	377.14	210	-43.5	168.5

The second identifier in the Hole ID (18, 19, or 20) indicates the year of collection. The third identifier is the hole number utilized in Figure 6.

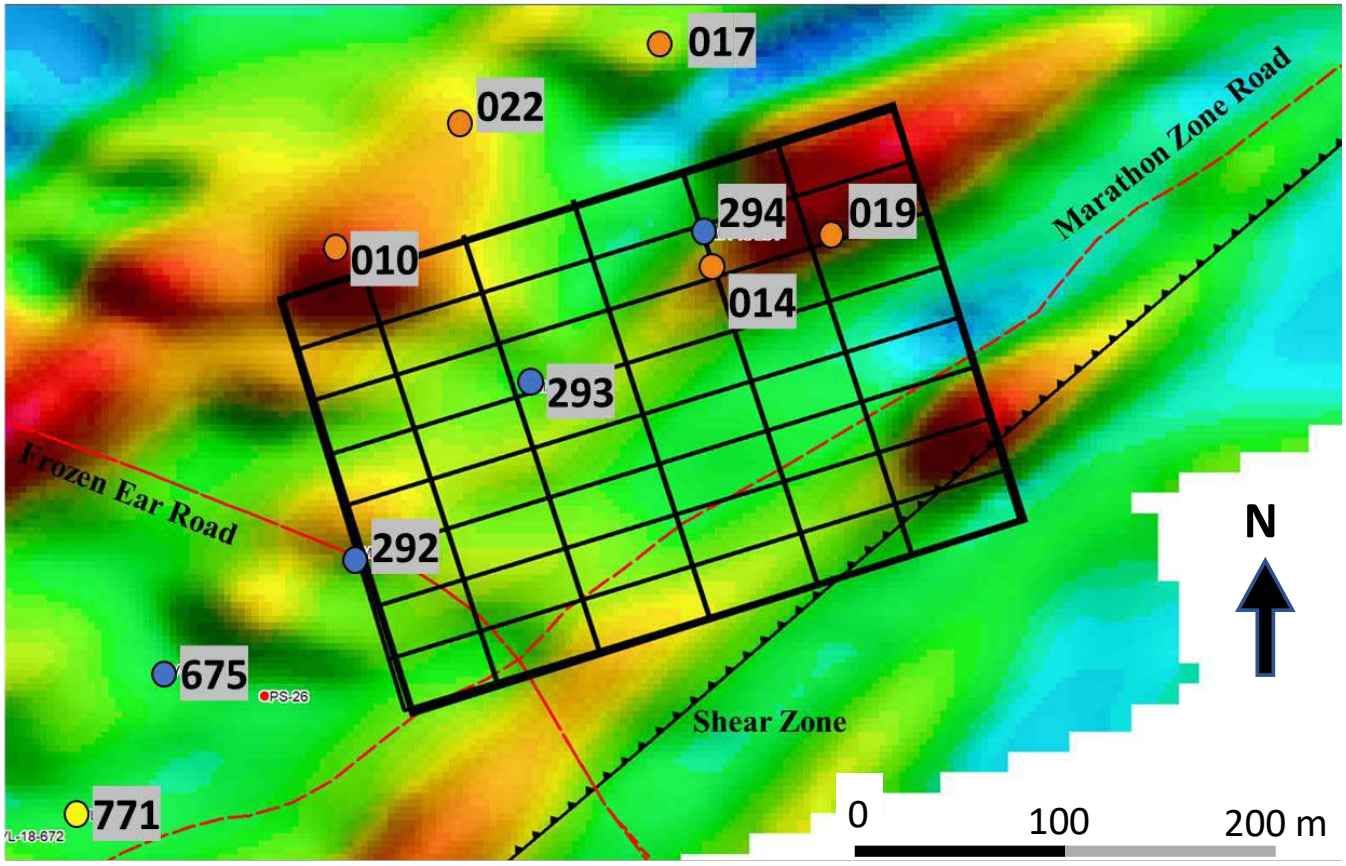

Figure 6. The 300 m x 200 m magnetic survey grid superimposed onto aeromagnetic data. The survey area is crossed by two main roads on the property which intersect at UTM NAD83 Zone 21U, coordinates 490820 mE, 5358935 mN. Drill collars (see Table 1) are shown by orange dots (drilled in 2018), a yellow dot (drilled in 2019) and blue dots (drilled in 2020).

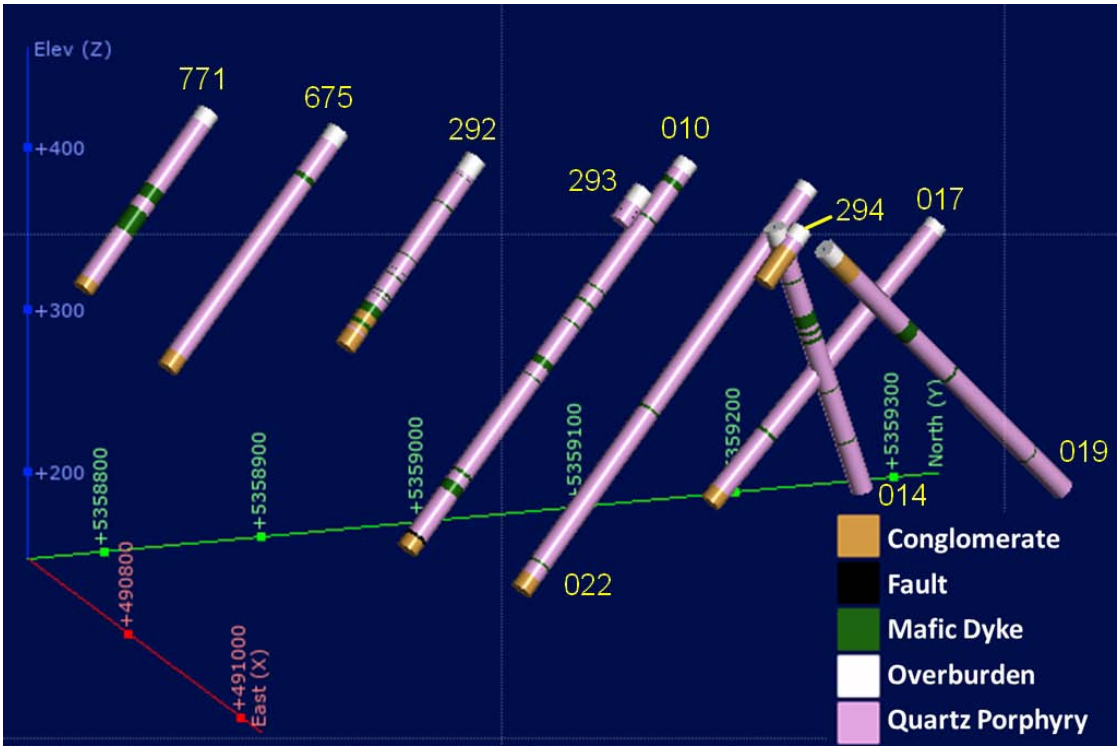

Figure 7. Drill holes with lithologies indicated. Profile is viewed at a plunge of 15, azimuth of 288. The northing direction is indicated by the green axis. Elevation (Z) is in metres above sea level. Model was created using Leapfrog Geo®.

FIELDWORK

The 200 m × 300 m survey grid was defined and marked prior to acquisition of magnetic data. A total of sixteen lines were done: nine 'X' lines oriented along the shear zone roughly WSW to ENE, 25 m apart, and seven perpendicular 'Y' lines oriented approximately SSE to NNW, 50 m apart (Figs. 5, 6). Two dirt roads cross the survey area: Frozen Ear Road and Marathon Zone Road (see also Fig. 1). Magnetic surveys were carried out along these roads in addition to the survey over the grid.

The survey was executed using a GEM GSM-19 Overhauser Magnetometer system, which included rover and base magnetic sensors and consoles (Fig. 8). Readings of total magnetic intensity (TMI), together with location information from a GPS receiver attached above the magnetic sensor (Fig. 8, left), were recorded every second, providing readings at intervals of approximately 65 cm.

The base sensor was set up on Frozen Ear Road, approximately 500 m northwest of the survey area, in a region where the magnetic field was flat and low. Readings of TMI were recorded there every 4 s. These data were later used to correct for variations of the local magnetic field over time.

The ground magnetic survey was completed over two days, August 8th and 9th, 2020. The lines Y = 0, X = 50, X = 200, and X = 300 were each traversed twice (in opposite directions) to confirm repeatability. Location information is accurate to within 3 m (Flanagan 2021). The terrain is heavily wooded with thick soil and moss cover. The traverse lines crossed large ditches, rocks, stumps, and fallen trees (Fig. 8, right) that had to be avoided and may account for some variation in the TMI measurements. In addition, the survey area contained many anthropogenic objects such as culverts, a fuel tank, and a truck, the locations of which are indicated by black triangles in Figure 9, as they were responsible for significant magnetic anomalies. The metal casings on the drill collars (open circles in Figure 9) also produced small magnetic anomalies, less obvious in Figure 9.

Magnetic susceptibility measurements were taken on outcrop with a handheld Terraplus KT-10 magnetic susceptibility meter (Terraplus 2020). Measurements made on drill core at an earlier time with the same instrument are also included.

MAGNETIC RESULTS

Based on the International Geomagnetic Reference Field (Geomagnetism Canada 2020), the total magnetic field strength was 51867 nT in this immediate area at the time of the survey. This value was subtracted from all total magnetic intensity measurements to find the residual magnetic

Figure 8. Left: First author with magnetometer. Right: magnetic survey terrain.

intensity (RMI). These data were then loaded, gridded, and mapped using Seequent's Oasis Montaj software. Filtering was computed using Oasis Montaj's MAGMAP extension to complete Reduction to Pole, which allowed removal of effects of magnetic declination and inclination, resulting in the RMI map in Figure 9. Details are provided in the figure caption. No information about remanent magnetization in these rocks is available, so remanence, if any, was not taken into account. Anthropogenic features are marked (black triangles, circles) so that their magnetic signatures can be recognized and discounted; for example, the strong anomalies near the southwestern corner of the grid, near the black triangles, are considered to be cultural noise. Subtler features associated with the drill collars (circles) do not affect interpretation of the map.

Two distinct patterns are seen on the map: linear features in the east and more irregularly shaped anomalies in the west. A linear magnetic high trends WSW in the northeastern corner of the map. A linear magnetic low occurs directly south, and then another magnetic high. An area of weakening strength can be seen in the centre of the map, which also corresponds to the distinct break in pattern. The linear features to the northeast are interpreted to correspond to mafic dykes with high magnetite content. The zone of weakening strength may be due to the oxidation of magnetite to hematite, which demagnetizes rocks and is common at fault and fracture zones (Dentith and Mudge 2014). A fault in this area, approximately perpendicular to the VLSZ, would explain the break in pattern.

MAGNETIC SUSCEPTIBILITY RESULTS

Magnetic susceptibility measurements were obtained from outcrop at eleven different locations on the property (Table 2); however, none are from the field area due to lack of outcrop. Of the eleven locations, seven are quartz porphyry (lighter pink unit in Figure 1), three of which contain mineralized QTP veins. The other readings are from two mafic dykes, a thick vein of quartz, and sedimentary rocks in the siliciclastic unit NW of the VLIS on the shore of Victoria Lake (Fig. 1). Ten measurements were taken at each location. Significant outliers were removed, and the geometric and arithmetic averages of each outcrop were taken (Table 2, Fig. 10).

A large spread in average magnetic susceptibility exists within and between the outcrops. Such variation is not unexpected, as rock magnetism depends on the concentration of accessory minerals which are commonly unevenly distributed. Measurements taken from drill core with the same instrument also showed a wide range and are in agreement with field samples (Fig. 10).

As expected, the quartz vein has very low magnetic susceptibility. In general agreement with drill core measurements, the sedimentary rock and the quartz porphyry (QP) have intermediate magnetic susceptibilities and the relatively unaltered dyke #1 has a high magnetic susceptibility. The QP with QTP veins has lower magnetic susceptibilities than QP without veins, likely due to the diluting effect of the QTP veins which contain less magnetite. It is also possible that magnetic susceptibility of the QP was reduced in the alteration halos of the QTP

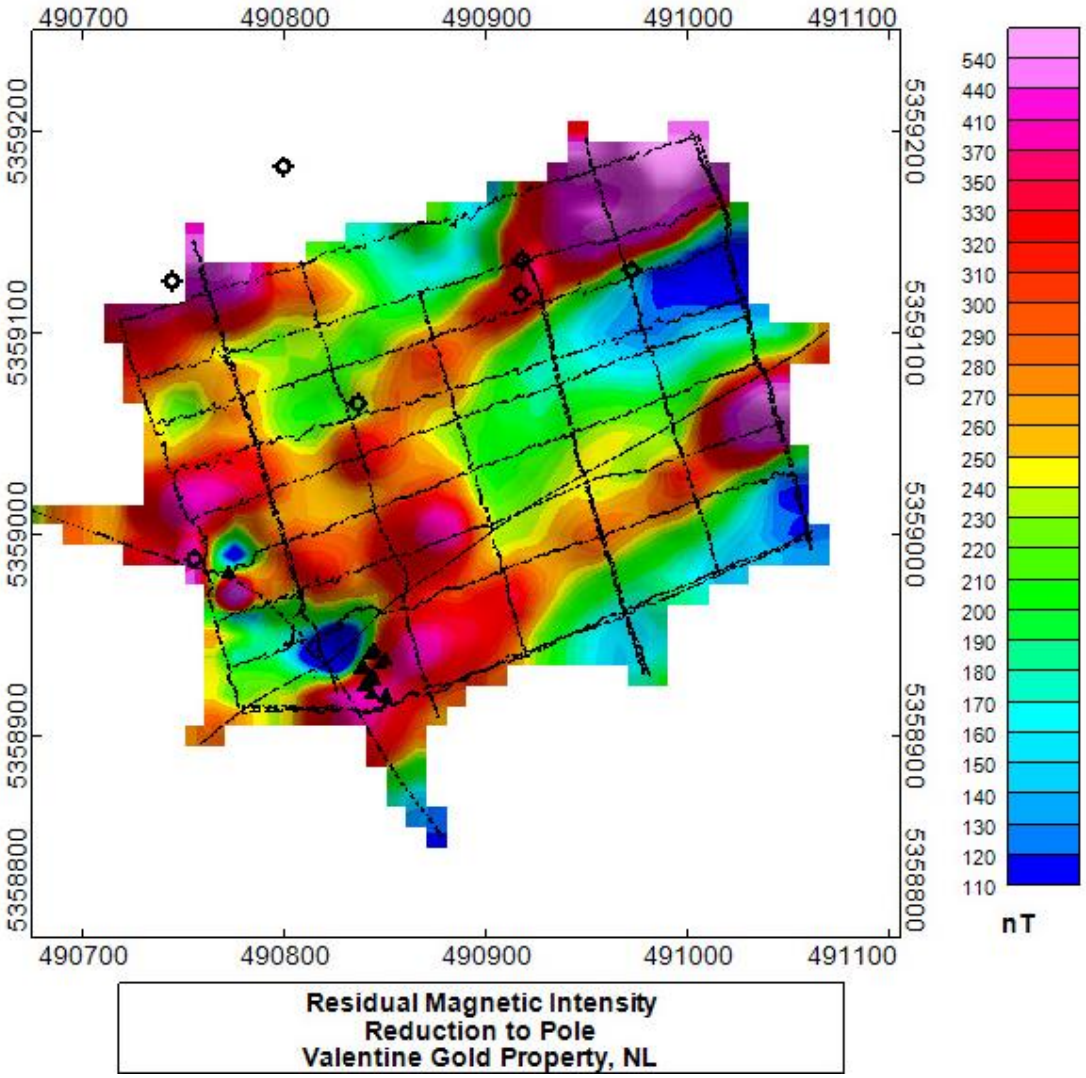

Figure 9. The residual magnetic intensity (RMI) map with reduction to the pole (RTP). The RTP filter utilized declination -18.37°, inclination 68.36°, and magnetic field strength 51867 nT, calculated for location 491061 mE, 5359001 mN, NAD 83 Zone 21U at elevation 412 m on August 8th 2020 (Geomagnetism Canada 2020). Circles = drill collars, triangles = anthropogenic objects. Gridding method is minimum curvature, cell size is 10 m, and the colour method is histogram normalized.

veins. Two types of alteration are observed in these halos: albitization/silicification and muscovite alteration (C. Samson, pers. comm. 2018). Both are associated with hydrothermal activity which could reduce magnetization in basalts (e.g., Szitkar *et al.* 2014; Runyon *et al.* 2019). The drill core susceptibility values for QP with QTP veins are mostly lower than those for the outcrops, perhaps because it is easier to distinguish this unit from the QP without QTP veins in drill core than in outcrop. Altered dyke #2 has a low magnetic susceptibility, lending support to the idea that enhanced alteration in the fault region could be responsible for the decreased magnetic intensity there.

MODELLING

In the computer program Leapfrog Geo®, the drill data (Fig. 7) were used to create a boundary surface between the QP and the conglomerate, representing the VLSZ. A single modelled boundary surface had a sharp bend in the northwestern corner (Flanagan 2021), so a better representation with two individual planes was modelled (Fig. 11). The two planes have different strikes and dips, providing further evidence that a fault exists, at a high angle to the shear zone. A displacement in the modelled surface can be interpreted as a brittle fault offsetting the shear zone in a sinistral sense (Fig. 12).

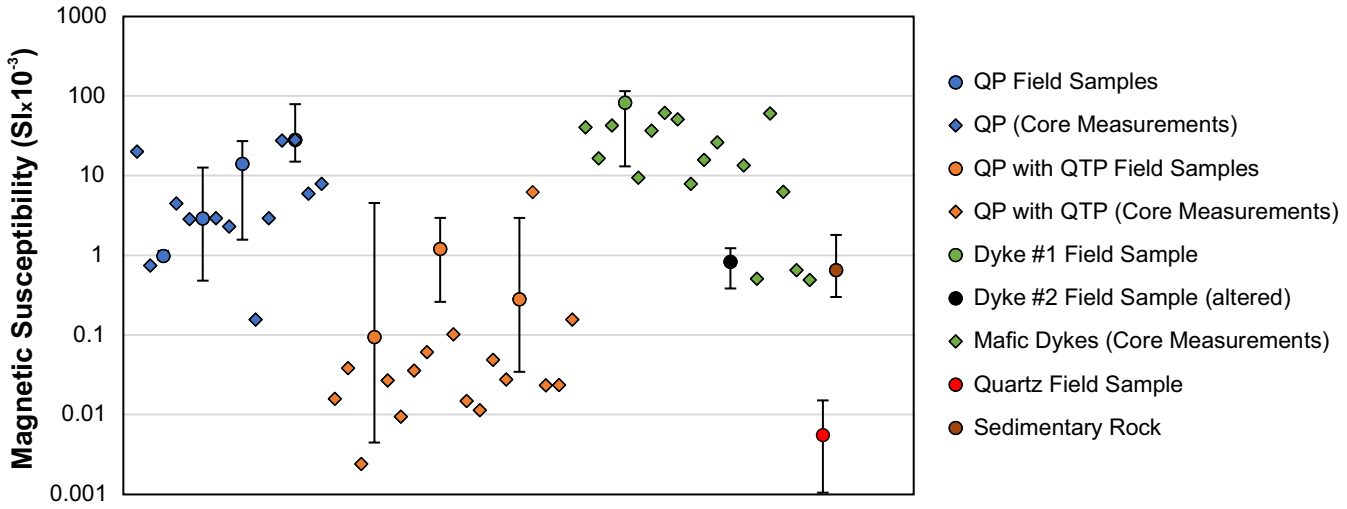

Figure 10. Average magnetic susceptibility values for outcrop and core samples, based on 10 measurements per outcrop/core. Standard deviations at 1σ. Note logarithmic scale. Circles = field samples, diamonds = drill core measurements. Bars on outcrop points indicate the standard deviation of the 10 measurements. Standard deviations for drill core measurements are similar.

The strikes and dips were calculated using standard three-point calculations (Table 3). From these values, an approximate offset of 100 m was calculated between the planes at the present surface level. The changes in the magnetic pattern and in the orientation of the conglomerate contact surface cannot be accounted for by strike slip alone, indicating that there is significant throw on the fault.

Figure 12 displays the traces of the conglomerate contact superimposed on the drill core data (left) and the magnetic data (right). The location and orientation of the fault are poorly constrained as it was intercepted only at one point, at the bottom of drill hole 293 (Figs. 11, 12) at a slant depth of 24.5 m. Drill hole 022, which extends directly underneath drill hole 293 (as best seen in Figure 12), does not intercept the fault. One possible orientation for the fault trace that would fit these two constraints is N-S, as shown in Figure 12 (left). In this scenario, the fault dips to the east so that hole 022 does not intercept it at depth: a dip angle of 85° or less would accomplish this. An alternative fault trace is NW-SE between the traces of the shear zone, as shown in the right panel of Figure 12. This modelled fault trace better matches the break in pattern and area of weakened total magnetic intensity mentioned above; however, it requires the fault to bend to the north so that drill hole 022 does not intercept it. These two possibilities are sketched in the inset of Figure 4, showing that both are plausible fits to the larger-scale magnetic data.

Locations of mafic dykes in drill log data correspond with locations of magnetic highs, as seen in Figure 12. In particular, as indicated by the yellow ovals in the left panel, the thickest dyke intersections in the northeast correspond with strong magnetic highs. To see whether the magnetic signatures could be produced by mafic dykes with simple geometry and reasonable susceptibility, forward modelling was carried out using the 3D gravity/magnetic modelling software ModelVision®. Data were extracted along two lines 50 m apart across the NE part of the RMI map, where two linear magnetic highs are located, one on each side of the QP-conglomerate contact (Fig. 13). Mafic dykes responsible for the magnetic highs were modelled as tabular synthetic bodies with the same dip as the nearby shear zone contact and with uniform magnetic properties. To allow for the differing strength of the anomalies on lines 1 and 2, both dykes were split into two bodies, with thicknesses of 5 m (similar to drill core intercepts) and

Table 2. Field sample average magnetic susceptibility measurements (unitsSI×10^{-3}).

Sample	Easting (m)	Northing (m)	Arith Avg	Geom Avg	Standard Deviation
QP #1	486775	5355231	0.99	0.98	0.09
QP #2	489418	5358072	4.8	2.9	4.8
QP #3	490732	5359121	17	14	8
QP #4	490732	5359121	31	28	18
QP with QTP #1	486155	5356037	0.74	0.094	1.4
QP with QTP #2	486706	5355743	1.5	1.2	0.9
QP with QTP #3	486706	5355743	0.97	0.28	1.1
Dyke #1	486706	5355743	92	82	29
Dyke #2	490732	5359121	0.88	0.83	0.28
Quartz	490732	5359121	0.0077	0.0055	0.0052
Sedimentary Rock	480835	5355497	0.69	0.65	0.24

Based on 10 measurements per location, with arithmetic and geometric averages given. QP = VLIS quartz porphyry rock; QTP = quartz tourmaline pyrite veining. Dyke #2 is a 30 cm wide mafic dyke with chlorite alteration.

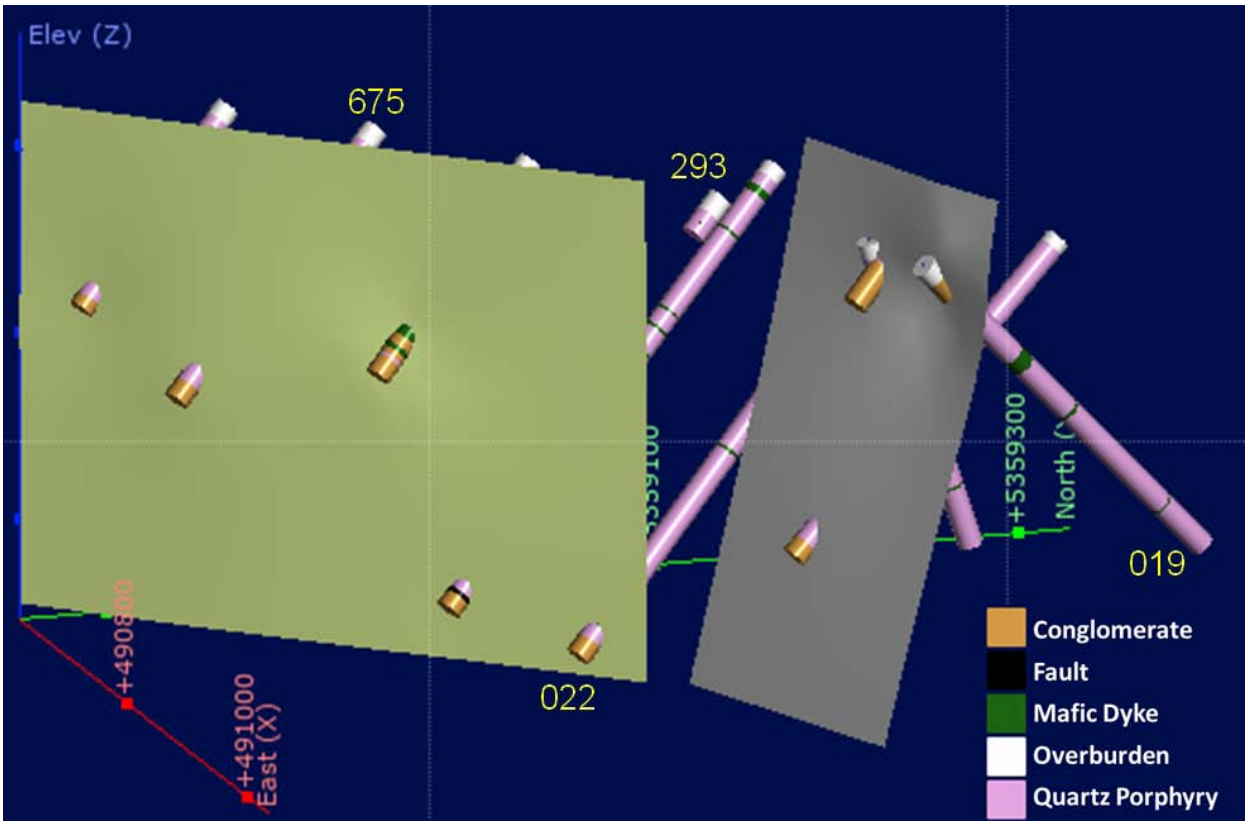

Figure 11. Drill holes with discontinuous modelled shear zone surface. The discontinuity is attributed to faulting of an original single surface. Profile is viewed at a plunge of 15, azimuth of 288, as in Figure 7. Model was created using Leapfrog Geo®.

Table 3. Strikes and dips of modelled shear zone surfaces.

Surface	Strike (°)	Dip (°)
SW surface	43.9	88.7
NE surface	71.6	78.2

a separation of 50 m. The lengths, depth to the top, and magnetic susceptibilities of the four bodies were modified to reproduce the observed magnetic anomalies (Table 4). The magnetic susceptibility of the surroundings was assumed to be negligible. Good agreement was found between models and measurements for dyke slant lengths of about 100 m (Fig. 10), except at the NW ends of the lines. This discrepancy is attributed to a third dyke, not included in the model but seen in NW dipping drill cores 014 and 019 (Fig. 7). The magnetic susceptibilities for the bodies fall within the measured range for mafic dykes (cf. Tables 2 and 4). The differences in the best fit magnetic susceptibilities for the four modelled bodies (4 to 19 SI×10^{-3}; Table 4) could reflect actual variations in the magnetic susceptibility of the dykes or they could be due to differences in the dyke thicknesses which were assumed to be 5 m in the models.

SUMMARY AND CONCLUSIONS

At the Valentine Lake Property, gold mineralization is mostly restricted to a quartz porphyry unit near a shear zone trending SW-NE. The shear zone contains a steeply dipping contact with a relatively barren conglomerate unit. This study was carried out in order to constrain the location of this contact (and therefore of the mineralization) in a region where a fault offset was suspected. Since the shear zone contains several mafic dykes orientated sub-parallel to the contact, a high-resolution magnetic survey was carried out over the region to delineate changes that could be related to faulting. This work was combined with magnetic susceptibility measurements of key units and drill core data. Mapping of the magnetic data using the

Table 4. Properties of modelled bodies. All bodies have width 50 m, thickness 5 m, and dip 78°.

Body	Susceptibility ($SI \times 10^{-3}$)	Depth to top (m)	Depth to base (m)	Azimuth (°)
1a	9.5	17	151.2	71
2a	7	23	107	71
1b	19	17	138.7	66.2
2b	4	18.5	100	66.2

software Oasis Montaj and modelling using the software Leapfrog Geo® and ModelVision® resulted in a consistent 3D structural model, including the strikes and dips of the contact on either side of a sinistral fault with an offset on the surface of about 100 m with two trace possibilities (Fig. 4, inset). The fault likely has significant throw based on sharp changes in strike and dip of the sheared contact and differences in the pattern of magnetization across the fault, differences which cannot be explained by 100 m of sinistral fault motion alone. A decrease in magnetic intensity in the fault region may be due to alteration of the mafic dykes.

ACKNOWLEDGMENTS

We thank Marathon Gold employees, in particular the Manager of Exploration, Nic Capps, for supporting this project, and Corey Caines and John Maloney for their assistance in the field. We also thank Stephanie Abbott for field assistance and general guidance, and to Peter Bruce, Sarah Greene, Regan Jacobson, and Miguel Shano for help with the various software packages used in this project. Detailed reviews from Karl Butler, an anonymous reviewer, and journal editors Aaron Bustard and Sandra Barr helped to substantially improve this manuscript.

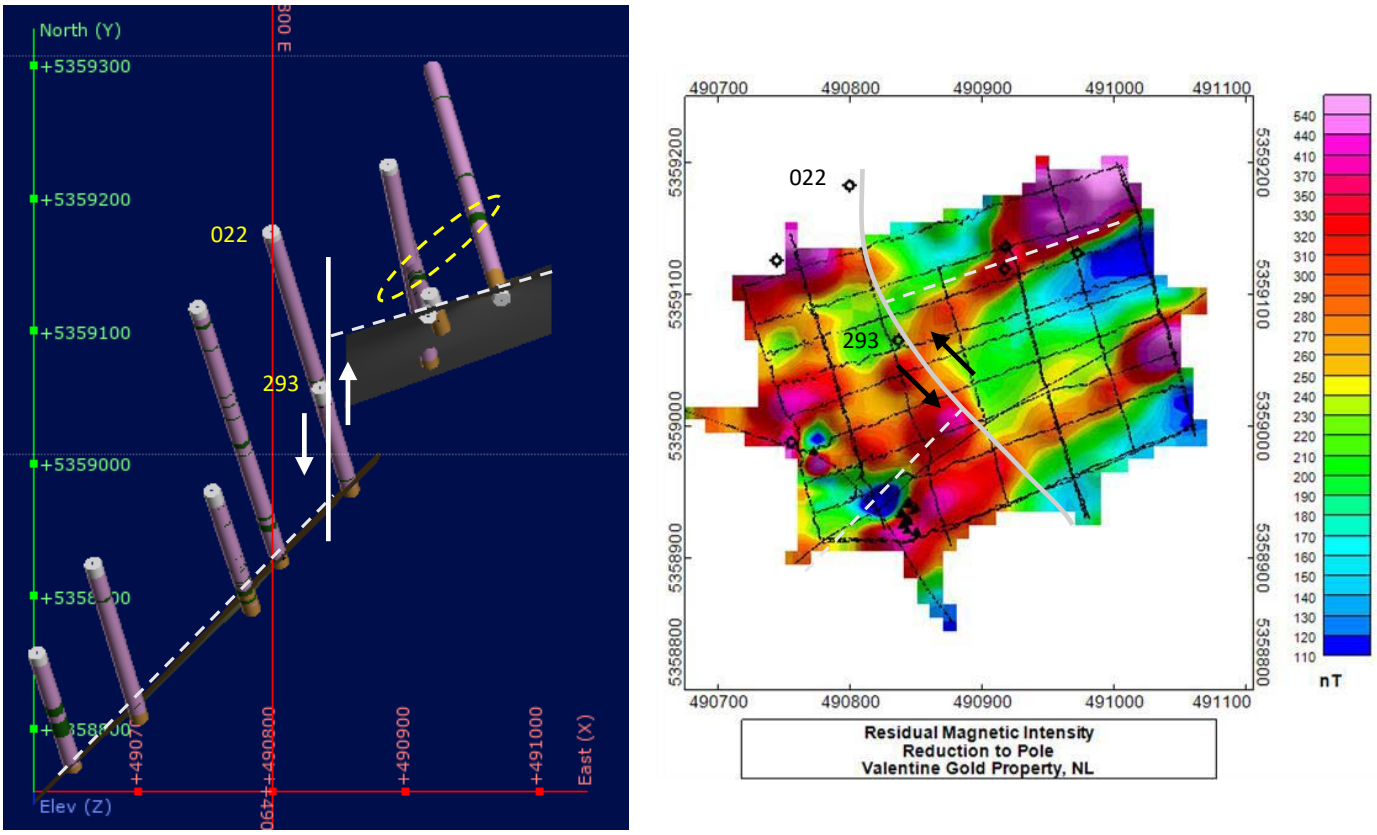

Figure 12. Drill data with modelled shear zone surface (left), compared with residual magnetic intensity map with modelled shear surface (right). White dashed lines show the trace of the shear zone, black dashed line shows the trace of the modelled fault, and black arrows show direction of movement. Yellow dashed oval shows correspondence between a mafic dyke intersection and a magnetic high.

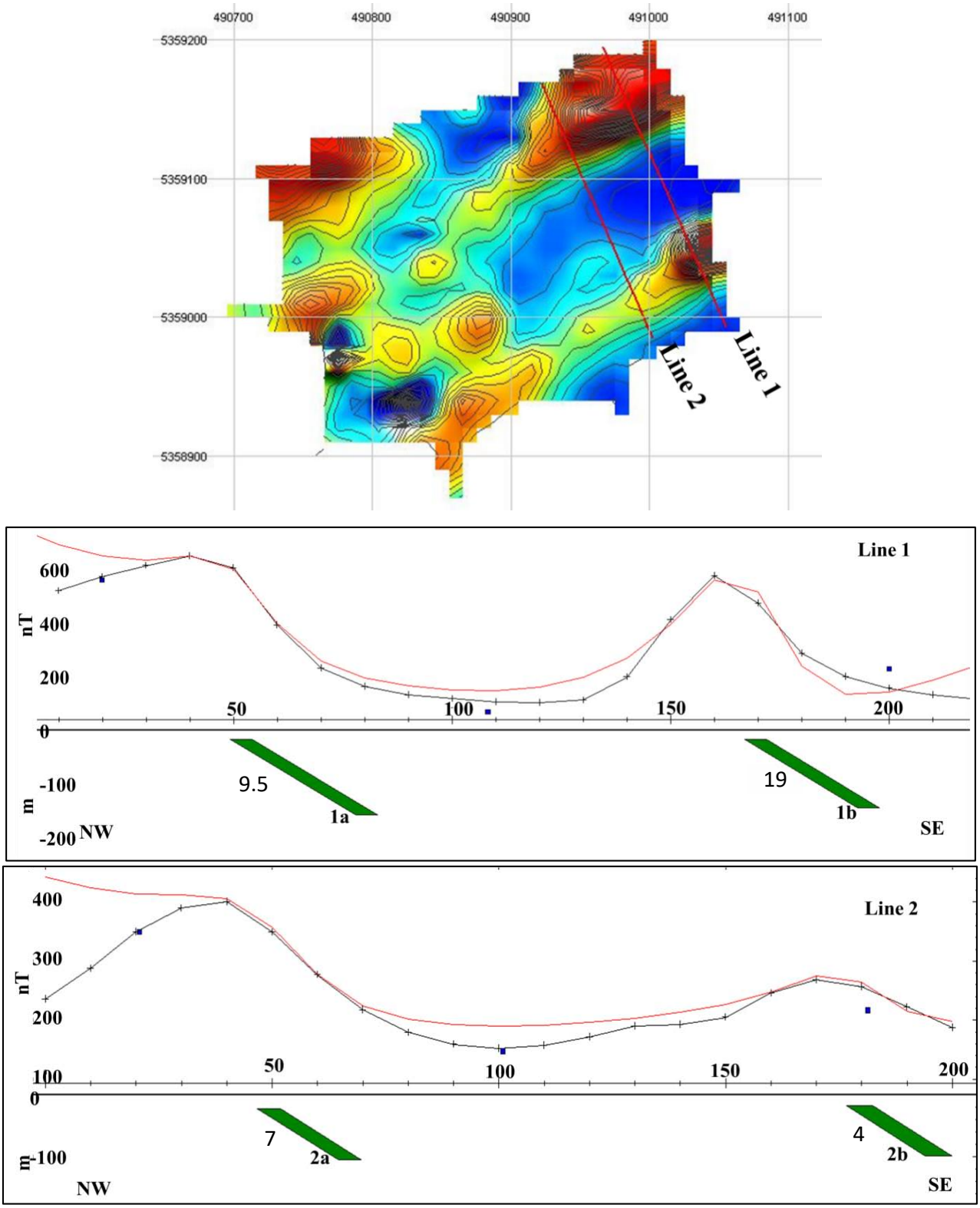

Figure 13. Magnetic modelling, created in ModelVision®. Top: map view showing locations of two profiles selected for modelling. Bottom: cross sectional view showing dyke bodies 5 m thick, dipping at 78 degrees (note different horizontal and vertical scales). Modelled bodies in green: numbers to the left are magnetic susceptibilities in units of SI×10^{-3} (for further physical properties see Table 4), black curve is RMI from data, red curve is the model.

REFERENCES

Dentith, M. and Mudge, S.T. 2014. Geophysics for the mineral exploration geoscientist. Cambridge University Press, 438 p. https://doi.org/10.1017/CBO9781139024358

Evans, D.T.W. and Kean, B.F. 2002. The Victoria Lake Supergroup, central Newfoundland – its definition, setting and volcanogenic massive sulphide mineralization. Newfoundland and Labrador Department of Mines and Energy, Geological Survey. Open File NFLD/2790, 68 p.

Evans, D.T.W., Kean, B.F., and Dunning, G.R. 1990. Geological studies, Victoria Lake Group, central Newfoundland. *In* Current Research, Newfoundland Department of Mines and Energy, Geological Survey Branch, Report 90-1, pp. 135–144.

Flanagan, M. 2021. Magnetics study within the Valentine Gold Property, Newfoundland. Unpublished B.Sc. Honours thesis, Memorial University of Newfoundland and Labrador, St. John's, Newfoundland and Labrador, Canada 73 p.

Geomagnetism Canada 2020. Magnetic declination calculator. URL <https://www.geomag.nrcan.gc.ca/calc/calc-en.php> 14 October 2020.

Guay, M., Riopel, J., Carrier, A., Dunsworth, S., Allou, B., Trudel, D., St-Jean, E., D'Amours, I., and Letourneau, O. 2007. Helicopter-borne magnetic, gamma-ray spectrometry and VLF geophysical survey NTS map sheets 12A/06 and 12A/07. Unpublished data acquisition report, Valentine Lake gold project, 377 p. URL <https://gis.geosurv.gov.nl.ca/geofilePDFS/ReceivedBatch46/012A_1447_Part2.pdf> 08 July 2021.

Honsberger, I.W., Bleeker, W., Kamo, S.L., Sandeman, H.A.I., Evans, D.T.W., Rogers, N., van Staal, C.R., and Dunning, G.R. 2022. Latest Silurian syntectonic sedimentation and magmatism and Early Devonian orogenic gold mineralization, central Newfoundland Appalachians, Canada: Setting, structure, lithogeochemistry, and high-precision U-Pb geochronology. Geological Society of America Bulletin, 134, pp. 2933–2957. https://doi.org/10.1130/B36083.1

Kruse, S. 2020. Structural analysis of the Valentine Gold Project. Marathon Gold Corp., Unpublished internal report Project#: 20-46-F. Terrane Geoscience. 46 p.

Marathon Gold 2021. Technical report & feasibility study on the Valentine Gold Project. URL <https://marathon-gold.com/site/uploads/2021/04/Valentine-Gold-43-101_FS-Report_FINAL_Apr23_R2.pdf> 08 July 2021

Marathon Gold 2022. Valentine Gold Project, deposits. URL <https://marathon-gold.com/valentine-gold-project/deposits/> 1 February 2022.

Melanson, D. and Parks, C. 2019. Marathon Gold: Valentine Mine. Final Report on Lidar Survey. Aethon Aerial Solutions, Burlington, ON. Marathon Gold unpublished internal report, 10 p.

Runyon, S.E., Seedorff, E., Barton, M.D., Steele-MacInnis, M., Lecumberri-Sanchez, P., and Mazdab, F.K. 2019. Coarse muscovite veins and alteration in porphyry systems, Ore Geology Reviews 113, pp. 1–32. https://doi.org/10.1016/j.oregeorev.2019.103045

Szitkar, F., Dyment, J., Choi, Y., and Fouquet, Y. 2014. What causes low magnetization at basalt-hosted hydrothermal sites? Insights from inactive site Krasnov (MAR 16°38'N). Geochemistry, Geophysics, Geosystems 15, pp. 1441–1451. https://doi.org/10.1002/2014GC005284

Terraplus. 2020. Magnetic Susceptibility Meters URL <https://terraplus.ca/product-details/magnetic-susceptibility-meters> 24 September 2020.

Tettelaar, T. and Dunsworth, S. 2015. Supplementary assessment report of diamond core drilling, prospecting, trenching, channel sampling, trench rehabilitation, geological trench mapping, line cutting, ground magnetometer survey, environmental studies, and road repair & maintenance, Valentine Lake Property, Central Newfoundland, NTS 12A/06. Unpublished data acquisition report, 981 p. URL <https://gis.geosurv.gov.nl.ca/geofilePDFS/Batch2019/012A_1761.pdf> 24 September 2020.

Tettelaar, T. and Dunsworth, S. 2016. Supplementary assessment report of diamond core drilling, line cutting, ground magnetometer survey, and road repair & maintenance, Valentine Lake Property, Central Newfoundland, NTS 12A/06. Unpublished data acquisition report, 160 p. URL <https://gis.geosurv.gov.nl.ca/geofilePDFS/Batch2019/012A_1805.pdf> 24 September 2020.

Valverde-Vaquero, P., and van Staal, C.R. 2002. Geology and magnetic anomalies of the Exploits–Meelpaeg boundary zone in the Victoria Lake area (central Newfoundland): regional implications. Newfoundland Department of Mines and Energy Geological Survey, Report 02-1, pp. 197–209.

Van Staal, C. and Valverde-Vaquero, P. 2001. Relationships between the Dunnage-Gander zones in the Victoria Lake-Peter Strides Pond area. Newfoundland Department of Mines and Energy Geological Survey, Report 2001-1, pp. 1–9.

Van Staal, C., Valverde-Vaquero, P., Zagorevski, A., Rogers, N., Lissenberg, C., McNicoll, V. 2005. Geology, Victoria Lake, Newfoundland and Labrador. Geological Survey of Canada, Open File 1667, scale 1:50 000. https://doi.org/10.4095/221287

Van Staal, C.R., Whalen, J.B., Valverde-Vaquero, P., Zagorevski, A., and Rogers, N. 2009. Pre-Carboniferous, episodic accretion-related, orogenesis along the Laurentian margin of the northern Appalachians. Geological Society, London, Special Publications, 327, pp. 271–316. https://doi.10.1144/SP327.13

White, S.E. and Waldron, J.W.F. 2022. Along-strike variations in the deformed Laurentian margin in the Northern Appalachians: Role of inherited margin geometry and

colliding arcs, Earth Science Reviews 226. https://doi. org/10.1016/j.earscirev.2022.103931

Williams, H. 1979. Appalachian Orogen in Canada. Canadian Journal of Earth Sciences, 16, pp. 792–807. https://doi.org/10.1139/e79-070

Williams, H., Colman-Sadd, S.P., and Swinden, H.S. 1988. Tectonic-stratigraphic subdivisions of central Newfoundland. *In* Current Research, Part B, Geological Survey of Canada, Paper 88-JB, pp. 91–98. https://doi.org/10.4095/122425

Editorial responsibility: Aaron Bustard and Sandra M. Barr